Revealing direction of coupling between neuronal oscillators from time series: Phase dynamics modeling versus partial directed coherence

Dmitry Smirnov[a)]
Saratov Branch of the Institute of RadioEngineering and Electronics, Russian Academy of Sciences, 38 Zelyonaya Street, Saratov, 410019, Russia

Bjoern Schelter, Matthias Winterhalder, and Jens Timmer
FDM, Freiburg Center for Data Analysis and Modeling, University of Freiburg, Eckerstrasse 1, 79104 Freiburg, Germany and Bernstein Center for Computational Neuroscience Freiburg, University of Freiburg, Hansastrasse 9a, 79104 Freiburg, Germany

The problem of determining directional coupling between neuronal oscillators from their time series is addressed. We compare performance of the two well-established approaches: partial directed coherence and phase dynamics modeling. They represent linear and nonlinear time series analysis techniques, respectively. In numerical experiments, we found each of them to be applicable and superior under appropriate conditions: The latter technique is superior if the observed behavior is "closer" to limit-cycle dynamics, the former is better in cases that are closer to linear stochastic processes. © *2007 American Institute of Physics*. [DOI: 10.1063/1.2430639]

Empirical characterization of coupling between oscillatory systems with different dynamical properties is an actively studied problem in the field of both linear and nonlinear time series analysis. In particular, neuronal oscillators represent an important class of systems for which systematical investigation of the problem is still lacking. Here, we reveal coupling directions between neuronal oscillators by using a linear, partial directed coherence, and a nonlinear, phase dynamics modeling, time series analysis techniques for various spiking and bursting regimes and different types of coupling. Conditions of applicability and superiority for both techniques are formulated. Phase dynamics modeling appears the most efficient tool for studying dynamics close to a limit-cycle behavior, while partial directed coherence is superior when a nonlinear structure is distorted by noise. The former technique allows analysis of shorter time series but is less robust to dynamical noise influence.

I. INTRODUCTION

Interaction between neuronal systems at the single-cell level,[1,2] as well as at the levels of mesoscopic neuronal populations[3–5] and macroscopic brain structures,[6–8] has been actively studied over the last decades. In particular, synchronization phenomena in neuronal populations have often been in the center of attention[1–3,6,9] due to their relevance for investigating information processing in the brain, motor control, or pathological dynamical states such as epilepsy. Detection of weak directional couplings in ensembles of neuronal oscillators from their time series is of comparable importance.[10] The notion of "weak" coupling is relative. Here, it is relevant to understand it as "insufficient to induce a stable synchronization regime." Appropriate analysis techniques would reveal directionality and strength of information flow and thus localize "driving" and "driven" parts of

neuronal networks. The latter could be used, e.g., to localize epileptic foci[11] and to monitor restoration processes.[12] So far, this problem has been rarely addressed.[12,13] Phase dynamics modeling was used in Ref. 13 to reveal coupling between Hindmarsh-Rose oscillators that exhibited periodic spiking individually. Kiemel and co-authors[12] considered coupled bursting neurons under a specific hypothesis about distribution of spikes within a burst.

Our purpose here is to investigate possibilities of revealing directional couplings between two neuronal oscillators in a systematic manner. In particular, we consider various dynamical regimes such as spiking and bursting, including periodic, deterministically chaotic, stochastically perturbed, and noise-induced regimes. Furthermore, different types of coupling, such as linear and threshold coupling,[14] are investigated.

There is a number of techniques for the detection of directional coupling from time series. These analysis techniques can be subdivided into two major groups: (1) linear techniques—for instance, Granger causality,[15] directed transfer function,[16] partial directed coherence,[17,18] and (2) nonlinear ones—for instance, nearest neighbors statistics,[19,20] nonlinear Granger causality,[21] nonlinear cross-prediction,[22] phase dynamics modeling.[23,24] Any of these techniques can be used for the analysis of neuronal oscillators. However, such an application is often not straightforward. Linear techniques are well established and many of their properties are derived analytically, including significance levels. However, they are developed in the framework of linear stochastic processes and observed empirically to be applicable in the case of weak nonlinearity,[18] while neuronal spiking and bursting dynamics are highly nonlinear. Nonlinear state space techniques[20–22] may not be applied without modifications since state space vectors reconstructed via the delay embedding follow rather complicated orbits due to temporal non-

uniformity of the spiking or bursting dynamics. One of the very promising and sensitive techniques based on phase dynamics modeling[23,24] is justified for quasiharmonic oscillators with moderate phase nonlinearity.[25] For neuronal dynamics, the phase can be easily defined in the case of periodic spiking, in contrast to the noise-induced spiking or bursting regimes (see Sec. III B).

Therefore, conditions for practical applicability of different analysis techniques to neuronal oscillators and their relative superiority require a special investigation. Here, we analyze the performance of two time series analysis techniques exemplarily: partial directed coherence (PDC) and phase dynamics modeling (PDM). Both techniques give estimators of the coupling strengths equipped with significance levels which is of special importance for practical applications. Both techniques have already shown their efficiency for several practical examples.[18,25–28]

The paper is organized as follows. Section II describes several mathematical models of neurons used here as test examples. Section III comprises some details of both coupling estimation techniques and methodology of our investigation. The results are presented in Sec. IV and are discussed in Sec. V.

II. NEURON MODELS

Various conductance-based neuron models have been introduced that typically take the form of ordinary nonlinear differential equations of dimension in the range 2–6,[29–32] where one variable stands for a membrane potential and others for ionic currents. Roughly speaking, a common feature of those models is that they have fast as well as slow variables. The fast variables describe the membrane potential and, possibly, some of the ionic currents. The slow variables represent the rest of the ionic currents.[14] As a consequence, the neuron models are characterized by pulselike time realizations of the membrane potential. These systems are nonlinear and can exhibit a variety of dynamical regimes.

They can be excitable, i.e., generate a pulse (spike), only in response to a sufficiently strong perturbation. Deterministic neuron models can also exhibit regimes of periodic, quasiperiodic, and chaotic spiking. Excitable systems under the influence of considerable noise can show repetitive noise-induced spiking, typically with quite irregular interspike intervals (ISIs). However, subsequent ISI values may have the least variance for some intermediate noise level so that the dynamics are similar to a moderately perturbed periodic spiking.[33–35] Such an effect is called "coherence resonance."[33] The other possible type of neuron dynamics is called "bursting" (see, e.g., Refs. 14 and 36). Spikes are organized into short sequences (bursts) separated with comparatively long intervals of quiescence; i.e., interburst intervals (IBIs). The bursting can also be periodic, chaotic, etc. Numerous types of spiking and bursting regimes are classified based on bifurcations of the quiescent state and of a limit cycle involved.[14]

Two physiologically motivated ways of coupling between neurons are usually considered:[14,37,38]

- Linear diffusive coupling which models electrotonic coupling via gap junction. The function f, which determines the type of coupling, takes the form

$$f(x_1, x_2) = x_2 - x_1, \tag{1}$$

where x_1 and x_2 stand for the membrane potentials of the two neurons. The function $f(x_1, x_2)$ determines the influence of the x_2 dynamics on x_1. This type of coupling is typically considered as bidirectional and symmetric.[14]

- Unidirectional step-like (threshold) coupling, which models chemical synapse behavior.[39] The coupling function reads

$$f(x_1, x_2) = h(x_2)(x_{th} - x_1), \tag{2}$$

where x_1 and x_2 stand for the membrane potentials of the postsynaptic and presynaptic neurons, respectively, $h(x_2)$ is, e.g., the Heaviside function or hyperbolic tangent function modeling threshold response, x_{th} is a certain constant that is high and positive for excitatory coupling and can be set negative for inhibitory coupling.

Sometimes, unidirectional linear coupling is used as a simpler model of synaptic connections (see, e.g., Ref. 40). The coupling function then reads

$$f(x_1, x_2) = x_2. \tag{3}$$

This description captures just the fact of the dependence of the post-synaptic neuron dynamics on the membrane potential of the presynaptic neuron x_2.

In the following, we consider all these types of coupling and select neuron models representing different dynamical regimes: periodic spiking including the case of stochastic perturbations, noise-induced spiking of excitable systems, as well as periodic and chaotic bursting. We consider periodic spiking resulting from different bifurcations of a quiescent state. This is of particular interest since phase dynamics of neuronal oscillators are known to depend on the kind of the bifurcation involved.[14]

A. Classical FitzHugh-Nagumo oscillator

The first example is a classical FitzHugh-Nagumo (FHN) oscillator[30] where the limit cycle underlying periodic spiking arises via supercritical Andronov-Hopf bifurcation (see, e.g., Ref. 33). The equations for two coupled FHN oscillators are given by

$$\varepsilon_1 \dot{x}_1 = x_1 - x_1^3/3 - y_1 + k_1 f(x_1, x_2),$$

$$\dot{y}_1 = x_1 + a_1 + D\xi_1(t),$$

$$\varepsilon_2 \dot{x}_2 = x_2 - x_2^3/3 - y_2 + k_2 f(x_2, x_1), \tag{4}$$

$$\dot{y}_2 = x_2 + a_2 + D\xi_2(t),$$

where $\xi_i(t)$ are independent sources of Gaussian white noise with zero mean: $\langle \xi_i(t)\xi_i(t')\rangle = \delta(t-t')$. The parameter D denotes noise intensity and parameters a_i determine a dynamical regime of an individual oscillator. For $|a_i| > 1$, the ith
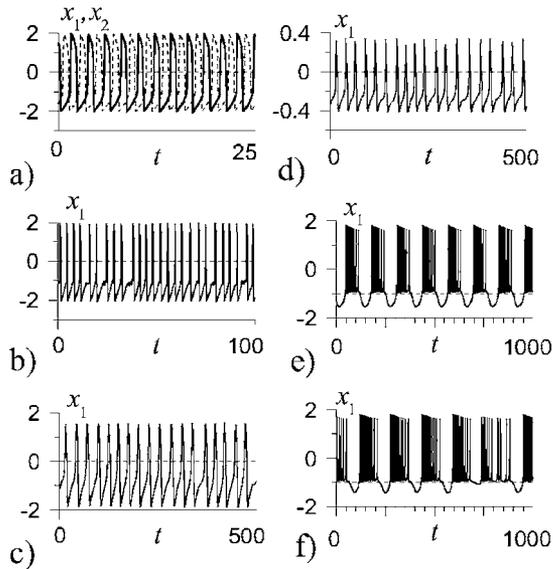
FIG. 1. Time series of neuron oscillators. Horizontal dashed lines show the threshold value used to define the phase. The latter is a quantity changed by 2π after each crossing of the threshold from below and linearly changing between crossings. (a) Unidirectionally coupled FHN oscillators Eq. (4) with linear coupling Eq. (3), $a_1=a_2=0.5$, $\varepsilon_1=0.01$, $\varepsilon_2=0.0095$, $D=0.02$, $k_1=0$, $k_2=0.001$. Solid line shows x_1, "oscillatory" dashed line, x_2. (b) Individual excitable FHN oscillator equation (4) in a coherent resonance regime, $a_1=0.5$, $k_1=0$, $D=0.02$. (c) Individual MFHN oscillator equation (5), $k_1=0$, $D=0.02$. (d) Individual ML oscillator equation (6), $k_1=0$, $D=0.005$. (e) Periodic bursting dynamics of an individual Hindmarsh-Rose oscillator equation (7), $I_1=2.7$, $D=0$. (f) Chaotic bursting dynamics of an individual Hindmarsh-Rose oscillator equation (7), $I_1=3.14$, $D=0$.

oscillator has a global fixed point attractor. When a_i passes the value of ± 1, the limit cycle appears. Typically, one considers $\varepsilon_i \ll 1$. In such a case, the variables x_i are fast and y_i are slow, leading to a kind of spiking behavior. The parameters ε_i determine the rate of relaxation of an individual oscillator to a nullcline $y_i=x_i-x_i^3/3$.[14] Hence, they affect the value of the limit cycle period. We chose $a_1=a_2=0.5$ to analyze periodic spiking [Fig. 1(a)] and $a_1=a_2=1.05$ to analyze noise-induced spiking [Fig. 1(b)] of excitable systems.

The noise-free FHN oscillators can be easily synchronized if their frequencies are similar, while their phase dynamics are almost independent of each other for strongly different frequencies that are not in a low-order resonant ratio. Therefore, we consider both the case of $\varepsilon_1 \approx \varepsilon_2$ and significantly different ε_i. The latter situation corresponds to different spiking frequencies of the interacting oscillators.

Parameters k_i govern the coupling strengths. If one of them is equal to zero, then the coupling is unidirectional.

B. Modified FitzHugh-Nagumo oscillator

The second example is a modified FitzHugh-Nagumo (MFHN) oscillator where the limit cycle arises via "saddle-node off invariant curve" bifurcation.[40] The equations read

$$\dot{x}_1 = x_1 - x_1^3/3 - y_1 + k_1 f(x_1, x_2),$$

$$\dot{y}_1 = \varepsilon_1[g(x_1) - y_1 - I_1 + D\xi_1(t)],$$

$$\dot{x}_2 = x_2 - x_2^3/3 - y_2 + k_2 f(x_2, x_1),$$

$$\dot{y}_2 = \varepsilon_2[g(x_2) - y_2 - I_2 + D\xi_2(t)],$$

where $g(u)=\alpha u$, $u<0$, and $g(u)=\beta u$, $u\geq 0$. The parameters were set to $\alpha=0.5$, $\beta=2.0$ following Ref. 40. The piecewise-linear function g causes a different kind of bifurcation, leading to periodic spiking as compared to the classical FHN system and, hence, different phase nonlinearity. In particular, MFHN oscillators can generate spikes whose width is much less than an ISI [Fig. 1(c)]. This property is close to a real neuron spiking.

Both classical and modified FHN oscillators exhibit Class 2 excitability;[14] i.e., repetitive spikes are generated in a certain frequency band and the basic frequency is relatively insensitive to a bifurcation parameter whose change leads to the appearance of the limit cycle underlying periodic spiking.

C. Morris-Lecar system

The third example represents Class 1 excitability; i.e., the spiking frequency tends to zero when the system is approaching the bifurcation point. Such a behavior is realized, e.g., by the Morris-Lecar (ML) system[31] where the limit cycle arises via "saddle-node on invariant curve" bifurcation at certain parameter values.[14,39] The equations are given by

$$\dot{x}_1 = I_1 - g_l(x_1 - V_l) - g_K y_1(x_1 - V_K)$$
$$- g_{Ca} m_\infty(x_1 - V_{Ca}) + k_1 f(x_1, x_2),$$

$$\dot{y}_1 = \lambda(x_1)[w_\infty(x_1) - y_1] + D\xi_1(t),$$

$$\dot{x}_2 = I_2 - g_l(x_2 - V_l) - g_K y_2(x_2 - V_K)$$
$$- g_{Ca} m_\infty(x_2 - V_{Ca}) + k_2 f(x_2, x_1),$$

$$\dot{y}_2 = \lambda(x_2)[w_\infty(x_2) - y_2] + D\xi_2(t),$$

where $m_\infty(u)=\frac{1}{2}[1+\tanh((u-V_1)/V_2)]$, $w_\infty(u)=\frac{1}{2}[1+\tanh((u-V_3)/V_4)]$, $\lambda(u)=\frac{1}{3}\cosh(u-V_3)/2V_4$, $V_1=-0.01$, $V_2=0.15$, $V_3=0.1$, $V_4=0.145$, $V_l=-0.5$, $V_K=-0.7$, $V_{Ca}=1.0$, $g_l=0.5$, $g_K=2.0$, $g_{Ca}=1.33$ [Fig. 1(d)]. The identical ML oscillators are known to be relatively difficult to synchronize even though their phase dynamics are mutually dependent.[14]

D. Hindmarsh-Rose oscillator

In order to analyze different bursting regimes, coupled four-dimensional Hindmarsh-Rose oscillators[41] with a unidirectional threshold coupling

$$\dot{x}_1 = y_1 + 3x_1^2 - x_1^3 - z_1 + I_1,$$

$$\dot{y}_1 = 1 - 5x_1^2 - y_1 - gw_1,$$

$$\dot{z}_1 = \mu[-z_1 + 4(x_1 + h) + D\xi_1(t)],$$

$$\dot{w}_1 = \nu[-w_1 + 3(y_1 + h)],$$

$$\dot{x}_2 = y_2 + 3x_2^2 - x_2^3 - z_2 + I_2 + k\frac{3.0 - x_2}{1 + e^{-50.0(n-4.0)}},$$

$$\dot{y}_2 = 1 - 5x_2^2 - y_2 - gw_2,$$

(5)

(6)

(7)

$$\dot{z}_2 = \mu[-z_2 + 4(x_2 + h) + D\xi_2(t)],$$

$$\dot{w}_2 = \nu[-w_2 + 3(y_2 + h)],$$

$$\dot{n} = \Theta(x_1 + 1.0)(x_1 + 1.0) - 0.05n,$$

are investigated, where $g = 0.0278$, $\mu = 0.00215$, $\nu = 0.0009$, $h = 1.605$, $l = 1.619$, and Θ is the Heaviside function. The differential equation for n is a more plausible model of a chemical synapse than the threshold coupling equation (2). For the parameter values given, the isolated neuron exhibits quiescent membrane voltage for $I_1 < 0.73$, bistability in state space near a subcritical Hopf bifurcation occurring at $I_1 = 0.82$, periodic bursting for $0.82 < I_1 < 3.0$ [Fig. 1(e)], chaotic bursting for $3.0 < I_1 < 3.25$ [Fig. 1(f)], and "continuous" chaotic spiking for $I_1 > 3.25$.

III. METHODS

A. Phase definition

The first step for any phase dynamics based approach is the estimation of instantaneous phases $\{\phi_1(t_i)\}$ and $\{\phi_2(t_i)\}$ from the time series $\{x_1(t_i)\}$ and $\{x_2(t_i)\}$, where $t_i = i\Delta t$ ($i = 1, \ldots, N$), Δt is the sampling interval. The most widespread techniques for the phase extraction are based on the analytic signal approach implemented via Hilbert transform[42] or complex wavelet transform.[43] However, they are not well suited for pulselike signals.

For the spiking dynamics, the phase of a signal can be defined as a quantity which is equal to $2\pi n$ when the value of x_i crosses a certain threshold from below for the nth time and linearly increases between two subsequent crossings. This is a phase related to spikes; we call it "spiking phase" and use the threshold value of $x_i = 0$ in all examples below to determine it [Figs. 1(a)–1(d)]. This definition is very robust in the case of only two neuronal oscillators, which is considered here, since the spikes can be easily detected even under significant measurement noise. Moreover, interspike intervals seem to carry all necessary information about the dynamics.

The PDM technique described in Sec. III B has already been shown to be applicable to deterministic neuronal oscillators individually exhibiting periodic spiking.[13] However, the "spiking phase" dynamics are essentially nonuniform in time for the bursting regimes. The phase increases rapidly within a burst and much slower between bursts. The phase dynamics exhibit strong diffusion for a chaotic bursting regime so that applicability of the PDM technique without any adaptations is questionable. It is important to note the difficulties of the analysis of bursting regimes when the phase is related to ISIs.

It is possible to consider a "bursting phase" as suggested in Ref. 12. However, the technique of Kiemel and co-authors involves rather time-consuming calculations; i.e., integration of the Fokker-Planck equation to evaluate the likelihood function, and a specific assumption about the character of spiking within a burst. In contrast, we use the threshold crossing technique in Sec. IV E, but with a lower threshold corresponding to the onset of a burst: the threshold value of

$x_i = -1$ [see Figs. 1(e) and 1(f)]. Such an approach is not appropriate for several systems since it may sometimes be difficult to distinguish between ISI and IBI. For the system investigated in Sec. IV E, however, distinction between ISI and IBI is clear. We check the behavior of both phase definitions in Sec. IV E.

B. Phase dynamics modeling

To identify coupling from the phases of two weakly coupled oscillators, Rosenblum and Pikovsky proposed to test whether the future time evolution of the phase of each oscillator is influenced by the phase of the other one.[23] For this purpose, one constructs a global model map

$$\phi_1(t + \tau) - \phi_1(t) = F_1[\phi_1(t), \phi_2(t)] + \xi_1(t),$$
$$\phi_2(t + \tau) - \phi_2(t) = F_2[\phi_2(t), \phi_1(t)] + \xi_2(t), \tag{8}$$

where $\phi_{1,2}(t)$ are unwrapped phases, τ is a finite interval, and $\xi_{1,2}$ are zero-mean random processes. F_1 is a trigonometric polynomial of the form

$$F_1(\phi_1, \phi_2) = \sum_{m,n} [a_{m,n}\cos(m\phi_1 + n\phi_2)$$
$$+ b_{m,n}\sin(m\phi_1 + n\phi_2)]. \tag{9}$$

F_2 is defined analogously. Equations (8) are the difference form of rather universal stochastic differential equations[44] describing the evolution of coupled phase oscillators and reflect the properties of a wide range of oscillatory processes. Following Refs. 23 and 24, we used third-order polynomials for $F_{1,2}$ and set τ equal to the minimal of the two basic oscillation periods for all numerical examples below.

The strength of the influence of the process x_2 on the process x_1 ($2 \rightarrow 1$) is defined as

$$c_1^2 = \frac{1}{2\pi^2} \int_0^{2\pi} \int_0^{2\pi} (\partial F_1/\partial \phi_2)^2 d\phi_1 d\phi_2. \tag{10}$$

It can be shown[24] that

$$c_1^2 = \sum_{m,n} n^2(a_{m,n}^2 + b_{m,n}^2). \tag{11}$$

When dealing with time series, one has to estimate the coefficients $a_{m,n}, b_{m,n}$, e.g., via the least-squares technique. The estimators $\hat{c}_1$ and $\hat{c}_2$ of the quantities c_1 and c_2 can then be derived by making usage of Eq. (11) with true coefficients values $a_{m,n}, b_{m,n}$ substituted by their least-squares estimates $\hat{a}_{m,n}, \hat{b}_{m,n}$. Here and throughout the paper, we supply with "hats" all the estimates obtained from time series. The estimators $\hat{c}_1$ and $\hat{c}_2$ are quite exact for long and stationary time series and become biased otherwise.[24] To remove this bias, we follow the approach of Ref. 24 and use the modified estimators $\hat{\gamma}_{1 \leftarrow 2}$ and $\hat{\gamma}_{2 \leftarrow 1}$ for the quantities c_1 and c_2 characterizing the influences $2 \rightarrow 1$ and $1 \rightarrow 2$, respectively (see the formulas in the appendix). Furthermore, $1.6\hat{\sigma}_{\hat{\gamma}_{i \leftarrow j}}$ is the 0.05 significance level for $\hat{\gamma}_{i \leftarrow j}$, i.e., the presence of the influence $j \rightarrow i$ is inferred from a time series if $\hat{\gamma}_{i \leftarrow j} > 1.6\hat{\sigma}_{\hat{\gamma}_{i \leftarrow j}}$, where the factor of 1.6 has been found empirically. The quantities $\hat{\gamma}_{i \leftarrow j}$ have skewed distributions, which

prevents an analytic derivation of their quantiles. The estimator of the variance $\hat{\sigma}_{\hat{\gamma}_{i\leftarrow j}}$ is derived based on the weighted sum of variances of polynomial coefficients estimators (see the appendix). Under the conditions of moderate coupling and moderate phase nonlinearity the modified estimators are unbiased in the case of relatively short time series covering about 50 basic periods or more.[25]

A reliable detection of the coupling direction can only be achieved in the nonsynchronous regime. If the coupling is strong enough to induce synchronization, the information about the coupling direction is lost, and the indices introduced above can take arbitrary values that are not related to the coupling intensity and direction. Hence, it is important to determine the overall degree of correlation between the phases of the two dynamics. For this purpose, we calculate the mean phase coherence

$$R = \sqrt{\langle\cos(\phi_1 - \phi_2)\rangle^2 + \langle\sin(\phi_1 - \phi_2)\rangle^2}, \qquad (12)$$

where angled brackets denote averaging over time.[6] It is symmetric in ϕ_1 and ϕ_2, attains the value of $R=1$ for the case of complete phase synchronization ($\phi_1 - \phi_2 = \text{const}$) and tends to zero for uncoupled oscillators. As we show in Sec. IV, a value of $R=0.75$ (sometimes even $R=0.5$) signifies the possibility of strong coupling and probable inconsistency of the PDM-based coupling estimators.

C. Partial directed coherence

Partial directed coherence is a parametric approach based on modeling multivariate dynamical systems by m-dimensional vector auto-regressive processes of model order p, abbreviated VAR[p]:

$$\begin{pmatrix} x_1(t) \\ \vdots \\ x_m(t) \end{pmatrix} = \sum_{r=1}^{p} \mathbf{a}_r \begin{pmatrix} x_1(t-r) \\ \vdots \\ x_m(t-r) \end{pmatrix} + \begin{pmatrix} \varepsilon_1(t) \\ \vdots \\ \varepsilon_m(t) \end{pmatrix}. \qquad (13)$$

$\varepsilon_i(t)$ are Gaussian white noise processes with covariance matrix $\mathbf{\Sigma}$. Estimating the elements $a_{kj,r}$ ($k,j=1,\ldots,m$, $r=1,\ldots,p$) of the coefficient matrices $\mathbf{a}_r$ is the basic step of partial directed coherence analysis. Below, we consider only the case of $m=2$.

Modeling the multivariate systems by vector auto-regressive processes is related to the causality term introduced by Granger.[15] Granger causality defines causal interactions in terms of predictability. The process X_j does not Granger-cause another process X_i with respect to all other processes if the linear prediction of $X_i(t+1)$ based on the past and present values of all variables, but X_j cannot be improved by adding the past and present values of X_j.

Partial directed coherence has been introduced as a frequency-domain measure for Granger causality.[17] The difference between the m-dimensional identity matrix I and the Fourier transform of the coefficients

$$\mathbf{A}(\omega) = I - \sum_{r=1}^{p} \mathbf{a}(r)e^{-i\omega r} \qquad (14)$$

leads to the definition of *partial directed coherence*:

$$|\pi_{i\leftarrow j}(\omega)| = \frac{|\mathbf{A}_{ij}(\omega)|}{\sqrt{\sum_k |\mathbf{A}_{kj}(\omega)|^2}}. \qquad (15)$$

Normalized between 0 and 1, a direct interaction from process X_j to process X_i is inferred by a nonzero partial directed coherence $|\pi_{i\leftarrow j}(\omega)|$. Let us denote $\hat{\pi}_{i\leftarrow j}(\omega)$ as the estimator of $\pi_{i\leftarrow j}(\omega)$ obtained from Eq. (15) with $\mathbf{A}_{kj}(\omega)$ replaced by its estimate $\hat{\mathbf{A}}_{kj}(\omega)$. In order to test the statistical significance of the nonzero value of $\hat{\pi}_{i\leftarrow j}(\omega)$ in application to finite time series, critical values are used. The α-significance level for the estimator of partial directed coherence can be approximated by[18]

$$\left(\frac{\hat{C}_{ij}(\omega)\chi^2_{1,1-\alpha}}{N\sum_k |\hat{\mathbf{A}}_{kj}(\omega)|^2} \right)^{1/2}, \qquad (16)$$

where $\chi^2_{1,1-\alpha}$ is the $1-\alpha$ quantile of the χ^2-distribution with one degree of freedom and $\hat{C}_{ij}(\omega)$ is an estimate of the constant

$$C_{ij}(\omega) = \mathbf{\Sigma}_{ii}\left\{ \sum_{k,l=1}^{p} \mathbf{H}_{jj}(k,l)[\cos(k\omega)\cos(l\omega) \right.$$
$$\left. + \sin(k\omega)\sin(l\omega)] \right\}. \qquad (17)$$

$\mathbf{H}_{jj}(k,l)$ are entries of the inverse $\mathbf{H} = \mathbf{R}^{-1}$ of the covariance matrix $\mathbf{R}$ of the VAR process.[45]

D. Design of simulation study

The above-mentioned ordinary differential equations for noise-free systems are integrated with the aid of Runge-Kutta-Verner fifth-order and sixth-order method to obtain time series of a necessary length N for different values of coupling strength. An adaptive step size was used to provide an error lower than 10^{-6} over a sampling interval. In the presence of dynamical noise, the Euler integration scheme with a fixed step size equal to $0.01\Delta t$ is used. The values of the sampling interval Δt vary for different examples and are reported below.

We use $N=30\,000$ data points in all examples below that corresponds to 1000–1500 interspike intervals. Those relatively long signals are needed to apply partial directed coherence reasonably since it requires sufficiently high-order p to describe power spectrum of pulse signals with a linear VAR model accurately. In this study, we chose the model order to be $p=500$. We compare both techniques by applying them to each time series and checking whether they give correct conclusion about coupling character. Namely, two conditions are examined:

(1) A technique should not give more false positive conclusions about the coupling than determined by the significance level.
(2) A technique is desired to give a high probability of positive conclusion about the presence of coupling if the latter is really present.

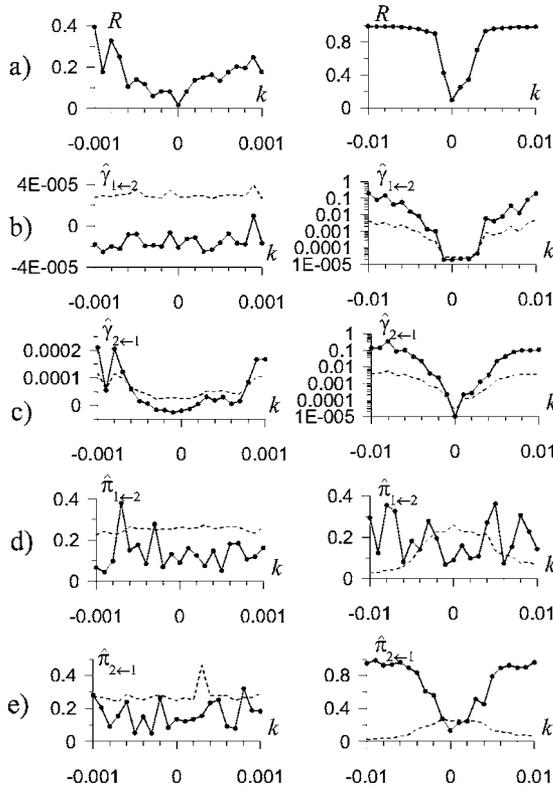The former condition is compulsory. Otherwise, an analysis

FIG. 2. Analysis of unidirectional linear coupling Eq. (3) between classical FHN oscillators in a stochastically perturbed periodic regimes with similar spiking frequencies. (a) Mean phase coherence. (b),(c) PDM coupling estimators (bold lines) and their significance level (dashed lines). True value of c_1^2 is zero. (d),(e) PDC estimates (bold lines) with 5% significance level (dashed lines).

technique is unreliable. As for the second condition, the probability to detect true coupling depends on the coupling strength, noise level, and time series length. For each technique, we find a range of coupling coefficient values where

each of the two conditions is fulfilled. Thereby, we compare, in particular, the sensitivity of the techniques to weak coupling.

IV. NUMERICAL RESULTS

A. Classical FitzHugh-Nagumo oscillators

The first investigation deals with the classical FitzHugh-Nagumo system with parameters $a_1 = a_2 = 0.5$, corresponding to a periodic spiking regime of an individual noise-free oscillator. We take a sampling interval $\Delta t = 0.1$, which corresponds approximately to 20 data points per interspike interval. In Fig. 2 we present the results for a moderate noise level $D = 0.02$, similar values of time constants $\varepsilon_1 = 0.01$ and $\varepsilon_2 = 0.0095$, and a unidirectional linear coupling [cf. Eq. (3)] with $k_1 = 0$ and $k_2 = k$. The values of all the estimates are shown versus coupling strength k for a single-trial experiment.

An almost phase synchronized regime ($R > 0.75$) is established both for excitatory coupling ($k \geq 0.004$) and inhibitory one ($k \leq -0.002$) [Fig. 2(a)]. $\hat{\gamma}_{1 \leftarrow 2}$ is not significantly different from zero, as indicated by its confidence interval in the range $-0.002 < k < 0.004$ [Fig. 2(b)], and it becomes spuriously "significantly" nonzero when the degree of phase synchrony is high (see also Tables I and II, the first row). The value of $\hat{\gamma}_{2 \leftarrow 1}$ becomes nonzero for excitatory coupling strength $k \approx 0.0008$ and inhibitory coupling strength $k \approx -0.0007$ [Fig. 2(c)]. In what follows we call such a minimal reliably detected coupling strength the "sensitivity threshold." Thus, the PDM technique works well in the intervals $(-0.002, -0.0007]$ and $[0.0008, 0.004)$. For the PDC corresponding intervals are $(-0.003, -0.002]$ and $[0.002, 0.005)$ [Figs. 2(d) and 2(e)].

We note that an "intuitively nonsignificant" small value of $\hat{\gamma}_{2 \leftarrow 1} \approx 0.0001$ for $k = 0.0008$ [Fig. 2(c)] is indeed significant. Moreover, this result is intuitively understandable. $\hat{\gamma}_{2 \leftarrow 1}$

TABLE I. Numerical results for excitatory coupling. We present the values of coupling coefficient for which: (1) true coupling is reliably detected, $k^{(1)}$; (2) presence of response-drive influence is erroneously detected for unidirectional scheme, $k^{(2)}$; (3) R exceeds the value of 0.75, $k^{(3)}$. The first value of $k^{(1)}$ and $k^{(2)}$ corresponds to the PDM technique, the second value to PDC.

Systems	$k^{(1)}$	$k^{(2)}$	$k^{(3)}$
1. FHN, unidir. coupling Eq. (3), $\varepsilon_1 = 0.01$, $\varepsilon_2 = 0.0095$, $D = 0.02$	0.0008, 0.002	0.004, 0.005	0.004
2. FHN, unidir. coupling Eq. (3), $\varepsilon_1 = 0.01$, $\varepsilon_2 = 0.05$, $D = 0.02$	0.003, 0.005	0.08, 0.08	0.08
3. FHN, unidir. coupling Eq. (18), $\varepsilon_1 = 0.01$, $\varepsilon_2 = 0.0095$, $D = 0.02$	0.003, 0.005	0.007, 0.01	0.007
4. FHN, bidir. coupling Eq. (1), $\varepsilon_1 = 0.01$, $\varepsilon_2 = 0.0095$, $D = 0.02$	0.0006, 0.003	0.002, 0.005	0.002
5. MFHN, unidir. coupling Eq. (3), $D = 0.02$	0.0004, 0.002	0.02, 0.03	0.02
6. MFHN, unidir. coupling Eq. (18), $D = 0.02$	0.001, 0.002	>0.1, 0.1	>0.1
7. ML, unidir. coupling Eq. (18), $D = 0.005$	0.004, 0.01	0.01, 0.1	>0.1
8. HR, Eq. (7), $I_1 = 3.04$, $I_2 = 3.14$, $D = 0.02$	0.001, 0.002	0.006, >0.01	>0.01
9. HR, Eq. (7), $I_1 = 3.04$, $I_2 = 3.14$, $D = 0$	0.0006, 0.0006	0.005, >0.01	>0.01
10. HR, Eq. (7), $I_1 = 2.7$, $I_2 = 2.5$, $D = 0.02$	0.0001, never	0.001, –	0.001

TABLE II. Numerical results for inhibitory coupling. Notation is the same as in Table I.

Systems	$k^{(1)}$	$k^{(2)}$	$k^{(3)}$
1. FHN, unidir. coupling Eq. (3), $\varepsilon_1=0.01$, $\varepsilon_2=0.0095$, $D=0.02$	$-0.0007, -0.002$	$-0.002, -0.004$	-0.002
2. FHN, unidir. coupling Eq. (18), $\varepsilon_1=0.01$, $\varepsilon_2=0.0095$, $D=0.02$	$-0.002, -0.003$	$-0.005, -0.007$	-0.005
3. MFHN, unidir. coupling Eq. (3), $D=0.02$	$-0.0003, -0.002$	$-0.04, -0.04$	-0.04
4. MFHN, unidir. coupling Eq. (18), $D=0.02$	$-0.001, -0.002$	$-0.02, -0.04$	-0.02
5. ML, unidir. coupling Eq. (18), $D=0.005$	$-0.005, -0.01$	$-0.008, -0.1$	< -0.1
6. HR, unidir. coupling Eq. (7), $I_1=3.04$, $I_2=3.14$, $D=0.02$	$-0.001, -0.005$	$-0.007, <-0.01$	< -0.01
7. HR, unidir. coupling Eq. (7), $I_1=3.04$, $I_2=3.14$, $D=0$	$-0.0006, -0.0006$	$-0.005, <-0.01$	< -0.01
8. HR, unidir. coupling Eq. (7), $I_1=2.7$, $I_2=2.5$, $D=0.02$	-0.0001, never	$-0.001, -$	-0.001

is, roughly speaking, the estimate of the squared "coupling intensity" in the difference equation (8). Thus, such a coupling intensity is about $\sqrt{\hat{\gamma}_{2 \leftarrow 1}} \approx 0.01$. If one divides this value by 2π [mean value of the phase increment on the left-hand side of Eq. (8)], one gets "relative coupling intensity" of the order 10^{-3} in correspondence with the order of $k = 0.0008$ [the latter can also be considered as relative coupling intensity since the oscillation amplitude is of the order of 1; see Fig. 1(a)].

The PDM technique turns out to be more sensitive in this example. This is not surprising since phase is well defined for these almost periodic spiking signals and the phases of coupled systems with similar frequencies interact efficiently.[14] However, the sensitivity thresholds of both techniques become closer to each other with increasing noise level. For lower noise levels, the PDM becomes more and more superior in terms of sensitivity. Finally, for the deterministic case $D=0$, the PDM can detect almost arbitrary weak coupling, while the PDC cannot reveal coupling at all, indicating that no conclusion about coupling presence can be drawn. The latter holds true for all noise-free settings throughout Sec. IV. Besides, one can observe in Fig. 2 that the PDC loses its efficiency for a stronger coupling than the PDM. In other words, the PDC can correctly reveal coupling character for regimes closer to phase synchronization when the PDM already fails. A possible explanation is that the former also extracts information from oscillation amplitudes, not only phases.

To consider the case of significantly different spiking frequencies, we specify $\varepsilon_1=0.01$ and $\varepsilon_2=0.05$ providing the ratio of frequencies $f_1/f_2 \approx 1.35$. The results are qualitatively similar to Fig. 2 (not shown). However, quantitative differences are present (see Table I, second row). For the excitatory coupling, sensitivity threshold of the PDM technique becomes $k \approx 0.003$; i.e., much higher than for the previous case. This is in agreement with theoretical results[14] stating that the phase dynamics become effectively less interdependent for different spiking frequencies. The sensitivity threshold of the PDC is $k \approx 0.005$. Both PDM and PDC fail for $k \geq 0.08$ due to high R-values ($R > 0.99$; R starts to exceed 0.75 for some k in the range 0.07–0.08).

For the similar spiking frequencies and unidirectional threshold coupling,

$$f(x_2, x_1) = \Theta(x_1)[1/(1 + e^{-x_1/0.1}) - 0.5](3.0 - x_2) \qquad (18)$$

instead of the linear one, the results are again qualitatively similar to Fig. 2 (not shown). Coupling of this type is also reliably detected by both techniques. However, their sensitivity is a bit worse since they catch only "the first moments" of the highly nonlinear coupling term (see Table I, third row, and Table II, second row). The PDM technique works well in the ranges of coupling $(-0.005, -0.002]$ and $[0.003, 0.007)$. The PDC detects coupling reliably in the ranges $(-0.007, -0.003]$ and $[0.005, 0.01]$. It is surprising that the PDC performance does not worsen strongly: PDC can describe only linear components of coupling, while this type of coupling is highly nonlinear.

Finally, diffusive coupling equation (1) ($k_1=k_2=k$, $D=0.02$, similar frequencies) is detected by both techniques, the domains of their applicability moving to weaker coupling. We considered only positive k, the results are similar to Fig. 2 (not shown; see Table I, fourth row). The PDM technique works in the range $[0.0006, 0.002)$, while the PDC does in $[0.003, 0.005)$. Note that the PDC starts to detect coupling when the PDM already fails. Moreover, mean phase coherence reaches the values of $R=0.98$ at $k=0.003$ that corresponds practically to phase synchronization. Therefore, in this example, PDC extracts useful information only from amplitudes.

B. Modified FitzHugh-Nagumo oscillators

The system equation (5) represents a different kind of bifurcation leading to periodic spiking behavior and, hence, may exhibit different phase dynamics properties. We specify $I_1=I_2=0.23$, $\varepsilon_1=0.2$, and $\varepsilon_2=0.3$ that provides individual periodic spiking regimes.[40] We investigate unidirectional coupling ($k_1=0$, $k_2=k$) and moderate noise $D=0.02$. The sampling interval is equal to 1.0, which corresponds again to 20 data points per interspike interval.

For the linear coupling equation (3), we obtained qualitatively the same results as in Fig. 2 (not shown; see Table I,

fifth row, and Table II, third row). The PDM is efficient for coupling ranges $(-0.04, -0.0003]$ and $[0.0004, 0.02)$. The sensitivity threshold for the PDM technique coincides with the classical FHN oscillators case by the order of magnitude; e.g., $k \approx 0.0004$ here and $k \approx 0.0008$ in the previous case for the excitatory coupling. Such a comparison makes sense since the amplitudes of the oscillations in both examples are approximately the same. The PDC is efficient in the ranges $(-0.04, -0.002]$ and $[0.002, 0.03)$. Thus, it is again less sensitive, but applicable for stronger couplings than the PDM technique.

The results for unidirectional threshold coupling Eq. (18) are again similar (not shown; see Table I, sixth row, and Table II, fourth row). Only quantitative differences are observed: the sensitivity thresholds increase. Thus, the PDM works in the ranges $(-0.02, -0.001]$ and $[0.001, 0.1]$, and 0.1 is just the last value of the interval checked. PDC is efficient in the ranges $(-0.04, -0.002]$ and $[0.002, 0.1]$. Here, not so typical superiority of the PDM for strong excitatory coupling is explained by low R-values for $k \leq 0.1$; e.g., $R = 0.5$ for $k = 0.1$. Synchronization takes place only for stronger coupling.

C. Morris-Lecar systems

This system represents Class 1 excitability at the values of parameters specified in Sec. II. Coupled identical systems of this type are difficult to synchronize despite the presence of interaction between their phases. Due to the absence of synchronization, it can be expected that coupling can be easily detected here.

We specify coupling of the form Eq. (18), $I_1 = I_2 = 0.075$, and the noise level $D = 0.005$. The noise level in absolute units is less than for the above examples, but oscillation amplitude in Morris-Lecar systems is also smaller so that the comparison of sensitivity thresholds by the order of magnitude makes sense. The sampling interval is equal to 1.0, which corresponds to approximately 25 data points per ISI (see Table I, seventh row, and Table II, fifth row). Results similar to Fig. 2 show that the PDM performs well in the ranges $(-0.008, -0.005]$ and $[0.004, 0.01)$, while the PDC is applicable in the ranges $(-0.1, -0.01]$ and $[0.01, 0.1]$. Thus, sensitivity of both techniques is not worse than for the previous examples of Class 2 excitability. Only in this particular case, PDM and PDC start to give erroneous conclusions when R is sufficiently low; i.e., PDM for $R \approx 0.2$ and PDC for $R \approx 0.5$. This exclusion should probably be ascribed to a specific nonlinearity of the system and coupling.

As an intermediate summary, we state that in the examples of periodic spiking including the cases of moderate stochastic perturbation (nonzero values of D), the PDM technique is applicable except for the situations corresponding to a considerable degree of phase synchrony, typically for $R > 0.75$. It is not surprising since it was developed for the dynamics close to a limit-cycle behavior. PDC is efficient only in noisy cases as it was developed for linear stochastic processes and imply mixing property of the investigated system. PDC is less sensitive for weak noise, but often performs well up to stronger coupling. However, it requires relatively
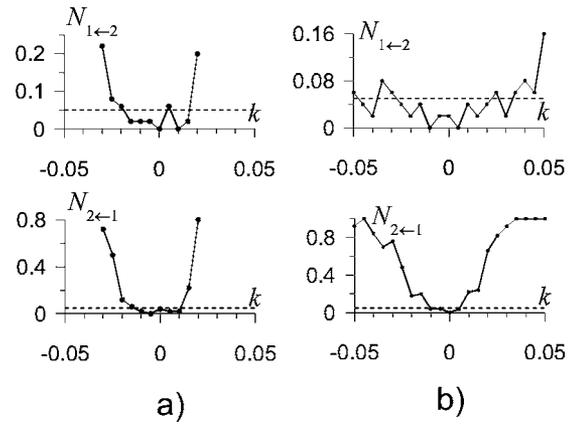

FIG. 3. Analysis of noise-induced spiking of FHN oscillators (4) in the coherence resonance regime ($D = 0.07$) over the ensemble of 50 realizations. (a) Relative numbers of conclusions about the presence of influence $2 \rightarrow 1$ ($N_{1 \leftarrow 2}$), $1 \rightarrow 2$ ($N_{2 \leftarrow 1}$) for the PDM technique. The dashed lines indicate the level of 0.05, which is a theoretically expected rate of erroneous conclusions if the technique works properly. (b) Relative numbers of different conclusions for PDC.

long time series to give reliable results. For example, PDC cannot reveal coupling at all for the time series length $N = 3000$ and the same other settings, while the sensitivity threshold of the PDM just becomes approximately three times as big as for $N = 30\,000$ (the sensitivity threshold of PDM is known to be inversely proportional to $\sqrt{N}$).[46]

D. Noise-induced spiking

Let us consider noise-induced spiking of excitable systems. Interspike intervals are usually rather irregular in such a case. However, for an intermediate noise level the ISI-values can exhibit the least variance (coherence resonance) so that the dynamical regime looks similar to stochastically perturbed periodic spiking. We use the classical FHN oscillator equation (4) with $a_1 = a_2 = 1.05$, $\varepsilon_1 = 0.01$, and $\varepsilon_2 = 0.0095$. Noise levels $D = 0.02$, $D = 0.07$, and $D = 0.25$ are examined. The second one corresponds to the coherence resonance regime[33] where the coefficient of variation of interspike intervals is minimal. Nonetheless, it is rather high as compared to weakly perturbed periodic spiking. In other words, phase diffusion is very strong.

Due to strong effect of noise for the fixed time series length used here, it is not meaningful to consider only single-trial experiments since the results are not similar to monotone plots of Fig. 1. The values of the estimates fluctuate strongly for different realizations of the same stochastic process. Therefore, we present the results averaged over an ensemble of 50 time series for each coupling value in Fig. 3. We consider unidirectional threshold coupling Eq. (18), $k_1 = 0$, $k_2 = k$. The sampling interval is equal to 0.1. For the noise level $D = 0.07$ it corresponds approximately to 40 data points per mean interspike interval.

The PDM technique performs relatively well only in a narrow range of coupling values $0.01 < k < 0.02$ and $-0.02 < k < -0.01$, where the number of wrong conclusions about the presence of influence $2 \rightarrow 1$ is below 5% in agreement with the expected theoretical properties of the estimator. The

number of correct conclusions is 5%–30% in that range [Fig. 3(b)]. Weaker coupling cannot be detected, stronger coupling leads to erroneously significant $\hat{\gamma}_{1 \leftarrow 2}$. The errors cannot be recognized using mean phase coherence which is always below 0.3 in this example. This is a quite undesirable feature of the PDM technique for analysis of such dynamics. PDC performs quite well as it does not give erroneous conclusions almost for the entire range of coupling examined and is more sensitive than the PDM technique. For example, the number of correct conclusions exceeds 5% for $k < -0.01$ and $k > 0.006$. It reaches 100% for $k \approx 0.035$. The unidirectional linear coupling equation (3) gives approximately the same results: All the plots are just a bit compressed along the k axis (not shown).

Different noise levels lead to more irregular interspike intervals.[33] Thus, for $D = 0.02$, the PDM is not applicable since it often gives erroneous conclusions and almost never determines the coupling character correctly. For a stronger noise $D = 0.25$, the PDM technique does not lead to errors but gives only an indefinite answer such that it is impossible to say anything about coupling. PDC is always applicable. Its sensitivity threshold decreases with noise level. Thus, the number of correct conclusions crosses 5% level at about $k = 0.004$ for $D = 0.02$ and $k = 0.03$ for $D = 0.25$.

The results can be explained intuitively. In essence, we consider the case that is not close to the limit-cycle behavior. It is a stochastic process with some nonlinear structure. Therefore, it is difficult to expect efficiency of the PDM technique. The situation is closer to a linear stochastic process than to a limit-cycle behavior; therefore, PDC should be suitable.

E. Bursting regimes

We analyze both periodic and chaotic bursting in Hindmarsh-Rose oscillator equation (7). The spiking phase, which can be defined here for a threshold value of the membrane potential equal, e.g., to 0.5, does not allow one to reveal coupling character using PDM either in chaotic or slightly perturbed periodic bursting regimes due to a strong phase diffusion. It takes place since there are alternating intervals of large and small spiking frequency. For spiking phase analysis, the PDM technique faces serious difficulties similar to the case of noise-induced spiking (Sec. IV D). Below, we define bursting phase using the threshold value of -1.0 [Figs. 1(e) and 1(f)].

The results for oscillators, which would individually exhibit chaotic bursting in a noise-free setting, are shown in Fig. 4, Table I, eighth row, and Table II, sixth row. The parameters values are $I_1 = 3.04$, $I_2 = 3.14$, and $D = 0.02$. The sampling interval is 2.0. There are approximately 200 data points per mean IBI. To analyze the bursting phase, we down-sampled the time series with sampling interval 20.0 providing 20 data points per a mean IBI. The results are shown in Fig. 4. The PDM technique works well in the ranges $(-0.007, -0.001]$ and $[0.001, 0.006)$. It starts to give spurious conclusions for $R = 0.5$ (at $k = -0.007$ and $k = 0.006$) in this example. PDC is a bit less sensitive; its domains of efficiency are $k \le -0.005$ and $k \ge 0.002$.
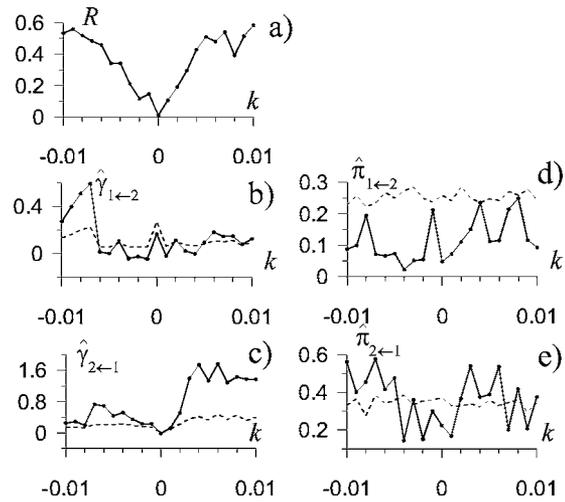

FIG. 4. Analysis of bursting dynamics in unidirectionally coupled Hindmarsh-Rose oscillator equation (7) individually exhibiting a stochastically perturbed chaotic bursting. (a) Mean phase coherence. (b),(c) PDM coupling estimators (bold lines) and their values corresponding to $p = 0.05$ (dashed lines) estimated from the same single time series. The true value of c_1^2 is zero. The phase is defined via IBIs. (d),(e) PDC estimators (bold lines) with 5% significance level (dashed lines).

By varying I_1 and I_2 in the range [3.04, 3.14], we observed quite similar results except for some quantitative differences. In the noise-free case, both PDM and PDC become more sensitive, for $I_1 = 3.04$, $I_2 = 3.14$ their thresholds are approximately the same and equal to -0.0006 and 0.0006, respectively. Again, the PDM technique starts to give spurious conclusions for $R = 0.5$ (at $k = -0.005$ and $k = 0.005$; see Table I, ninth row, and Table II, seventh row.

Stochastically perturbed periodic bursting is investigated for $I_1 = 2.7$, $I_2 = 2.5$, and $D = 0.02$. The PDM technique is very sensitive; it performs well in the ranges $(-0.001, -0.0001]$ and $[0.0001, 0.001)$; see Table I, tenth row, and Table II, eighth row. PDC is not applicable. Mixing is not strong enough so that even more IBIs (longer time series) is required in order that the PDC would have chances to reveal coupling correctly.

Thus, we showed that the PDM technique works well for bursting oscillators if the phase is related to IBIs. The PDM technique is more sensitive than the PDC for (stochastically perturbed) periodic bursting. For the time series length specified, the PDC is applicable only for chaotic bursting where stronger mixing takes place.

We should note that there are also more difficult cases when the isolated neuron oscillator demonstrates continuous chaotic spiking. In such a case, a weak interaction is not detectable with the PDM for a reasonable time series length since the phase diffusion is rather high; approximately as high as for the noise-induced dynamics of the classical FHN oscillator in the coherence resonance regime considered above. Stronger coupling may induce chaotic bursting regime in a driven oscillator.[41] In the latter case, it becomes even more difficult to analyze interactions between the oscillators. For instance, the use of the spiking phase for the driving oscillator and the bursting phase for the driven one may lead to biased estimators due to essentially different time

scales of the spiking and bursting dynamics. However, we would guess that it is efficient to use spiking phase only within simultaneous bursts. In this case, intervals of slow increase in spiking phase are ignored and phase dynamics are uniform as desirable for the PDM technique. If bursting neurons under investigation would represent Class 2 excitability and Class 2 spiking, then such spiking phase should be sensitive to weak coupling since spike synchronization is easily achieved for such systems.[14]

V. CONCLUSIONS

We have shown that both the *nonlinear* phase dynamics modeling technique and the *linear* partial directed coherence are able to detect directional couplings between neuronal oscillators reliably in various situations. However, both analysis techniques have different conditions of applicability since they are based on extraction of different features of the dynamics. For instance, partial directed coherence does not suit well for analysis of short time series where phase dynamics modeling can be easily applied.

The phase dynamics modeling technique is very efficient for periodic spiking or slightly perturbed periodic spiking. It faces serious difficulties for noise-induced spiking; analogous problems arise for the analysis of bursting regimes, if the phase is defined via interspike intervals. However, the technique appears applicable and very sensitive in the latter case if the phase can be defined via interburst intervals.

The partial directed coherence is not applicable in the case of individually periodic neuron dynamics. It is less sensitive than the phase dynamics modeling technique for weakly perturbed periodic spiking. Sensitivity thresholds for both techniques becomes closer to each other with increasing noise level. Partial directed coherence is efficient in cases of essential noise level or deterministic chaos since it is developed for linear stochastic processes and requires mixing property.

An interesting observation is that both techniques detect threshold coupling almost as easily as linear coupling.

The phase dynamics modeling technique is relatively tolerant to time series length and can be applied for time series as short as about 100 spikes. Partial directed coherence requires longer time series (about 1000 spikes) to give reliable results since it implies the use of high-order VAR models to reproduce power spectra of pulse signals and, hence, considerable amount of data is needed to estimate their coefficients reliably.

Both techniques cannot correctly reveal very strong coupling which induces synchronous regime. They become less efficient as "the degree of phase synchrony" increases. We note that partial directed coherence often performs well up to stronger coupling than the phase dynamics modeling technique. It is explained by the fact that partial directed coherence extracts some information from amplitudes, not only from phases. Note that both techniques can give false positive detection of influence of one oscillator on another one for strong unidirectional coupling (see Figs. 2–4). This situation can be diagnosed, e.g., by calculation of mean phase coherence. Roughly, if one gets $R > 0.75$ then the results of

coupling estimation cannot be considered as reliable (however, sometimes a value of $R = 0.5$ suggests the possibility of difficulties).

It might seem that both techniques work well only in a very narrow region of coupling intensities. However, the notions of weak and strong coupling are relative. In the examples considered here, synchronization takes place already for quite small absolute values of coupling coefficients. Both techniques work well typically for weaker couplings only. This is inevitable since directional coupling information is lost in the (nearly complete) synchronous regime. We call coupling strength leading to synchronization "strong coupling." Hence, the regions of applicability of both techniques are "almost up to strong coupling." What can be done in case of considerable phase synchrony when both techniques are erroneous will be investigated in the future work.

The other difficult situation for the PDM technique is the case of noise-induced spiking where $R < 0.3$ and the technique gives erroneous conclusions. To apply PDM in practice, the origin of spiking (perturbed limit-cycle or noise-induced behavior) should be assumed in advance. What can be done if one cannot state it with confidence will be investigated in the future as well. We believe that at this stage, it is useful just to take into account this difficulty.

We note, that generalization of the PDM technique to the case multiple interacting neurons is straightforward. One must just construct a phase dynamics model like Eq. (8), which involves phases of all those neurons. PDC is suitable for analysis of multiple systems by construction. Thus, we expect that our results concerning relative sensitivity of the techniques for the case of two neurons extends to bigger ensembles as well.

To summarize, the phase dynamics modeling technique is extremely sensitive when the neuronal dynamics are close to a limit-cycle behavior and the phase diffusion is not too high. Partial directed coherence is superior when nonlinear oscillatory structure of the dynamics is distorted to a significant extent by the dynamical noise. Both situations are widespread in applications to neuronal oscillators. In practice, it is reasonable to apply both techniques in combination to get more complete information about the character of the coupling scheme in neuronal systems.

APPENDIX: FORMULAS FOR THE PDM ESTIMATORS

Bias in, and variance of, $\hat{\gamma}_{1 \leftarrow 2}$ as the estimator of c_1^2 are related to variances of the least-squares coefficients estimators $\hat{a}_{m,n}, \hat{b}_{m,n}$. Under some simplifying assumptions of mod-

erate coupling and phase nonlinearity,[25] analytic expressions for them were derived.[24] Thus, the variance of the estimator $\hat{a}_{m,n}$ (except for $\hat{a}_{0,0}$) corresponding to the first equation in the set Eq. (8) is given by

$$
\hat{\sigma}_{\hat{a}_{m,n}}^2 = \frac{2\hat{\sigma}_{\xi_1}^2}{N}\left\{ 1 + 2\sum_{j=1}^{\tau/\Delta t-1}\left(1-\frac{j\Delta t}{\tau}\right)\cos\left[(m\hat{a}_{0,0}^{(1)}+n\hat{a}_{0,0}^{(2)})\frac{j\Delta t}{\tau}\right]\right.
$$

$$
\left. \times e^{-j(m^2\hat{\sigma}_{\xi_1}^2+n^2\hat{\sigma}_{\xi_2}^2)/2\tau}\right\},\tag{A1}
$$

where $\hat{a}_{0,0}^{(k)}$ stands for the estimates of the intercept in the kth equation $(k=1,2)$ of the set (8). Everything is analogous for $\hat{b}_{m,n}$ and for the second equation in Eq. (8).

Next, the estimator of $\sigma_{\hat{a}_{m,n}^2}^2$ reads

$$
\hat{\sigma}_{\hat{a}_{m,n}^2}^2 = \begin{cases} 2\hat{\sigma}_{\hat{a}_{m,n}}^4 + 4(\hat{a}_{m,n}^2-\hat{\sigma}_{\hat{a}_{m,n}}^2)\hat{\sigma}_{\hat{a}_{m,n}}^2, & \hat{a}_{m,n}^2-\hat{\sigma}_{\hat{a}_{m,n}}^2\geq 0, \\ 2\hat{\sigma}_{\hat{a}_{m,n}}^4, & \text{otherwise}. \end{cases}
$$

$$\tag{A2}$$

Finally, the expressions for $\hat{\gamma}_{1\leftarrow 2}$ and the estimator of its variance are as follows:

$$
\hat{\gamma}_{1\leftarrow 2} = \hat{c}_1^2 - \sum_{m,n}n^2(\hat{\sigma}_{\hat{a}_{m,n}}^2+\hat{\sigma}_{\hat{b}_{m,n}}^2),\tag{A3}
$$

$$
\hat{\sigma}_{\hat{\gamma}_{1\leftarrow 2}}^2
$$

$$
= \begin{cases} \sum_{m,n}n^4(\hat{\sigma}_{\hat{a}_{m,n}^2}^2+\hat{\sigma}_{\hat{b}_{m,n}^2}^2), & \hat{\gamma}_{1\leftarrow 2}\geq 5[\sum_{m,n}n^4(\hat{\sigma}_{\hat{a}_{m,n}^2}^2+\hat{\sigma}_{\hat{b}_{m,n}^2}^2)], \\ \frac{1}{2}\sum_{m,n}n^4(\hat{\sigma}_{\hat{a}_{m,n}^2}^2+\hat{\sigma}_{\hat{b}_{m,n}^2}^2), & \text{otherwise}. \end{cases}
$$

$$\tag{A4}$$

Everything is analogous for $\hat{\gamma}_{2\leftarrow 1}$ as the estimator of c_2^2.

[1]V. Makarenko and R. Llinas, Proc. Natl. Acad. Sci. U.S.A. **95**, 15747 (1998).
[2]E. Rossoni, Y. Chen, M. Ding, and J. Feng, Phys. Rev. E **71**, 061904 (2005).
[3]R. Larter, B. Speelman, and R. M. Worth, Chaos **9**, 795 (1999).
[4]P. A. Tass, *Phase Resetting in Medicine and Biology: Stochastic Modelling and Data Analysis* (Springer-Verlag, Berlin, 1999).
[5]P. A. Tass, T. Fieseler, J. Dammers, K. Dolan, P. Morosan, M. Majtanik, F. Boers, A. Muren, K. Zilles, and G. R. Fink, Phys. Rev. Lett. **90**, 088101 (2003).
[6]F. Mormann, K. Lehnertz, P. David, and C. E. Elger, Physica D **144**, 358 (2000).
[7]C. J. Stam and B. W. van Dijk, Physica D **163**, 236 (2002).
[8]F. Mormann, R. G. Andrzejak, T. Kreuz, C. Rieke, P. David, C. E. Christian, and K. Lehnertz, Phys. Rev. E **67**, 021912 (2003).
[9]H. D. I. Abarbanel, R. Huerta, M. I. Rabinovich, N. F. Rulkov, P. F. Rowat, and A. I. Selverston, Neural Comput. **8**, 1567 (1996).
[10]E. Pereda, R. Quian Quiroga, and J. Bhattacharya, Prog. Neurobiol. **77**, 1 (2005).
[11]R. Quian Quiroga, A. Kraskov, T. Kreuz, and P. Grassberger, Phys. Rev. E **65**, 041903 (2002).
[12]T. Kiemel, K. M. Gormley, L. Guan, T. L. Williams, and A. H. Cohen, J. Comput. Neurosci. **15**, 233 (2003).
[13]L. Cimponeriu, M. G. Rosenblum, T. Fieseler, J. Dammers, M. Schick, M. Majtanik, P. Morosan, A. Bezerianos, and P. Tass, Prog. Theor. Phys. Suppl. **150**, 22 (2003).
[14]E. M. Izhikevich, Int. J. Bifurcation Chaos Appl. Sci. Eng. **10**, 1171 (2000).
[15]C. Granger, Econometrica **37**, 424 (1969).
[16]M. Kaminski, M. Ding, W. A. Truccolo, and S. L. Bressler, Biol. Cybern. **85**, 145 (2001).
[17]L. A. Baccala and K. Sameshima, Biol. Cybern. **84**, 463 (2001).
[18]B. Schelter, M. Winterhalder, M. Eichler, M. Peifer, B. Hellwig, B. Guschlbauer, C. Läcking, R. Dahlaus, and J. Timmer, J. Neurosci. Methods **152**, 210 (2006).
[19]N. F. Rulkov, M. M. Sushchik, L. S. Tsimring, and H. D. I. Abarbanel, Phys. Rev. E **51**, 980 (1995).
[20]J. Arnhold, P. Grassberger, K. Lehnertz, and C. E. Elger, Physica D **134**, 419 (1999).
[21]U. Feldmann and J. Bhattacharya, Int. J. Bifurcation Chaos Appl. Sci. Eng. **14**, 504 (2004).
[22]S. J. Schiff, P. So, and T. Chang, Phys. Rev. E **54**, 6708 (1996).
[23]M. G. Rosenblum and A. S. Pikovsky, Phys. Rev. E **64**, 045202 (2001).
[24]D. A. Smirnov and B. P. Bezruchko, Phys. Rev. E **68**, 046209 (2003).
[25]D. A. Smirnov, M. B. Bodrow, J. L. P. Velazquez, R. A. Wennberg, and B. P. Bezruchko, Chaos **15**, 024102 (2005).
[26]M. G. Rosenblum, M. Camponeriu, A. Bezerianos, A. Patzak, and R. Mrowka, Phys. Rev. E **65**, 041909 (2002).
[27]I. I. Mokhov and D. A. Smirnov, Geophys. Res. Lett. **33**, L03708 (2006).
[28]M. Winterhalder, B. Schelter, J. Kurths, and J. Timmer, Signal Process. **85**, 2137 (2005).
[29]A. L. Hodgkin and A. F. Huxley, J. Physiol. (London) **117**, 500 (1952).
[30]R. FitzHugh, Biophys. J. **1**, 445 (1961).
[31]C. Morris and H. Lecar, Biophys. J. **35**, 193 (1981).
[32]J. L. Hindmarsh and R. M. Rose, Proc. R. Soc. London, Ser. B **221**, 87 (1984).
[33]A. S. Pikovsky and J. Kurths, Phys. Rev. Lett. **78**, 775 (1997).
[34]O. V. Sosnovtseva, A. I. Fomin, D. E. Postnov, and V. S. Anishchenko, Phys. Rev. E **64**, 026204 (2001).
[35]V. A. Makarov, V. I. Nekorkin, and M. G. Velarde, Phys. Rev. Lett. **86**, 3431 (2001).
[36]D. Terman, SIAM J. Appl. Math. **51**, 1418 (1991).
[37]G. B. Ermentrout and N. Kopell, SIAM J. Appl. Math. **50**, 125 (1990).
[38]R. E. Mirolo and S. H. Strogatz, SIAM J. Appl. Math. **50**, 1645 (1990).
[39]G. B. Ermentrout and N. Kopell, SIAM J. Appl. Math. **50**, 125 (1990).
[40]V. B. Kazantsev, V. I. Nekorkin, S. Binczak, S. Jacquir, and J. M. Bilbault, Chaos **15**, 023103 (2005).
[41]M. C. Eguia, S. P. Dawson, and G. B. Mindlin, Phys. Rev. E **62**, 7111 (2000).
[42]A. S. Pikovsky, M. G. Rosenblum, and J. Kurths, *Synchronization: A Universal Concept in Nonlinear Sciences* (Cambridge University Press, Cambridge, 2001).
[43]J. P. Lachaux, E. Rodgriguez, A. Le Van Quyen, A. Lutz, J. Martiniere, and F. Varela, Int. J. Bifurcation Chaos Appl. Sci. Eng. **10**, 2429 (2000).
[44]A. S. Pikovsky, M. G. Rosenblum, and J. Kurths, Int. J. Bifurcation Chaos Appl. Sci. Eng. **10**, 2291 (2000).
[45]H. Lütkepohl, *Introduction to Multiple Time Series Analysis* (Springer, New York, 1993).
[46]D. A. Smirnov and R. G. Andrzejak, Phys. Rev. E **71**, 036207 (2005).